Macromolecules

pubs.acs.org/Macromolecules
Article

Solving the Film Formation Dilemma: Blends of Soft Core−Hard "Shell" Particles

Hesham Abdeldaim, Edurne González, Noé Duarte, and José M. Asua*

Cite This: *Macromolecules* 2023, 56, 9054−9061
Read Online

ABSTRACT: The use of soft core−hard "shell" polymer particles is an alternative to overcome the film formation dilemma (achieving, at the same time, good film formation at a low temperature and good mechanical properties at a usually higher service temperature). In this article, blends of soft core−hard "shell" particles of different sizes have been prepared, and it has been observed that by adding tiny amounts of small particles (e.g., 1 wt %) to big particles, film formation can be substantially improved (lower minimum film formation temperature (MFFT) and higher critical cracking thickness (CCT)). Furthermore, mechanical properties of the films are also improved (higher elongation at break and toughness, maintaining Young's modulus and the stress at break) without affecting the water sensitivity of the film. It has been found that the viscoelastic properties of the small particles must be similar to those of the large ones in order to have a significant effect.

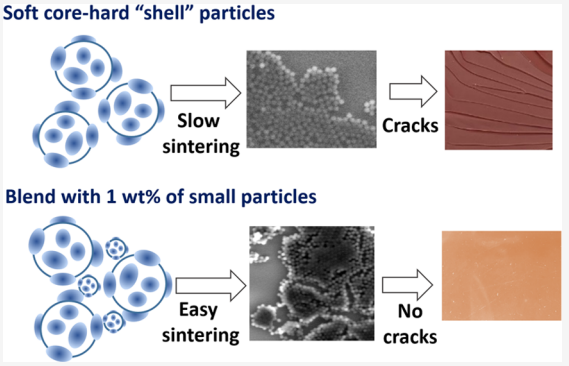

INTRODUCTION

Deceivingly unimportant, coatings play a significant role in the global economy (yearly corrosion losses account for almost 2% of the world's GDP[1]). Environmental concerns are pushing for the substitution of solvent-based coatings by waterborne ones.[2] Although waterborne coatings have the largest share of the market, the full substitution of solvent-based coatings in demanding applications has not yet been completely achieved. The reason is the so-called film formation dilemma of the waterborne coatings, that in order to form a good film, they need to have a low glass transition temperature (T_g), but to achieve good mechanical properties, a high T_g is needed. Out of the alternatives available to overcome this dilemma,[3−17] the use of latexes comprising a soft core covered by patches of a hard polymer (this morphology is referred to as soft core−hard "shell") is one of the more promising approaches.[12−17] The advantage with respect to a well-defined soft core−hard shell morphology is that the particles with a discontinuous shell deform more easily during film formation and yield a film morphology consisting of a honeycomb structure of the hard polymer filled with the soft polymer. However, although this structure results in very good mechanical properties,[12,15−17] the presence of a hard polymer at the surface of the particles increases the stress generated during film formation that often results in cracking,[17,18] which is catastrophic for substrate protection.[14,17] It is worth mentioning that cracking occurs more easily in thick films,[19] which are needed for demanding applications. Therefore, the ideal system should present low minimum film forming temperature (MFFT, minimum temperature at which a crack is not formed in the film), high critical cracking thickness (CCT, the maximum thickness of the coating for which no cracks appeared), and good mechanical and other application properties.

We recently reported on the effect of both the characteristics of soft core (T_g = 0 °C)−hard "shell" (T_g = 100 °C) latexes and the drying conditions on the stress generation and crack formation. This study led to the definition of the range of conditions to form a crack-free mechanically strong coating that can be cast at low temperatures.[17] In particular, small size (e.g., 90 nm in diameter) soft core−hard "shell" particles containing an acidic monomer in the formulation and 25 wt % of hard phase led to low MFFT (<5 °C), high CCT (1000 μm), and good mechanical properties at room temperature (Young's modulus = 5.2 MPa; stress at break = 10.5 MPa; elongation = 100%, hardness 3° Koening = 35 s). However, due to the relatively high concentration of surfactants used to stabilize the small particles, the films presented water sensitivity (water uptake = 11.25%), which is deleterious for substrate protection. In addition, the films cast from small particles presented some brittleness that may be a problem for some applications. Larger particles required lower concentrations of surfactants and hence were less sensitive to water. In addition, they presented a good balance

Received: September 19, 2023
Revised: October 30, 2023
Accepted: October 31, 2023
Published: November 13, 2023

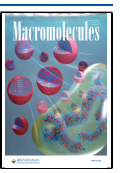

Table 1. Characteristics of the Soft Core/Hard "Shell" Latexes Prepared

latex	soft core		hard "shell"		dp (nm)*
	BA/MMA/S/AA (wt/wt %)	wt %	MMA/AA (wt/wt %)	wt %	
1	70/15/15/0	75	100/0	25	55
2	68/15/15/2	75	97/3	25	70
3	70/15/15/0	75	100/0	25	70
4	68/15/15/2	75	97/3	25	90
5	70/15/15/0	75	100/0	25	90
6	68/15/15/2	75	97/3	25	250
7	70/15/15/0	75	100/0	25	250
8	68/15/15/2	75	97/3	25	350
9	70/15/15/0	75	100/0	25	350
10	70/15/15/0	70	100/0	30	359

*dp: average particle diameter measured by DLS.

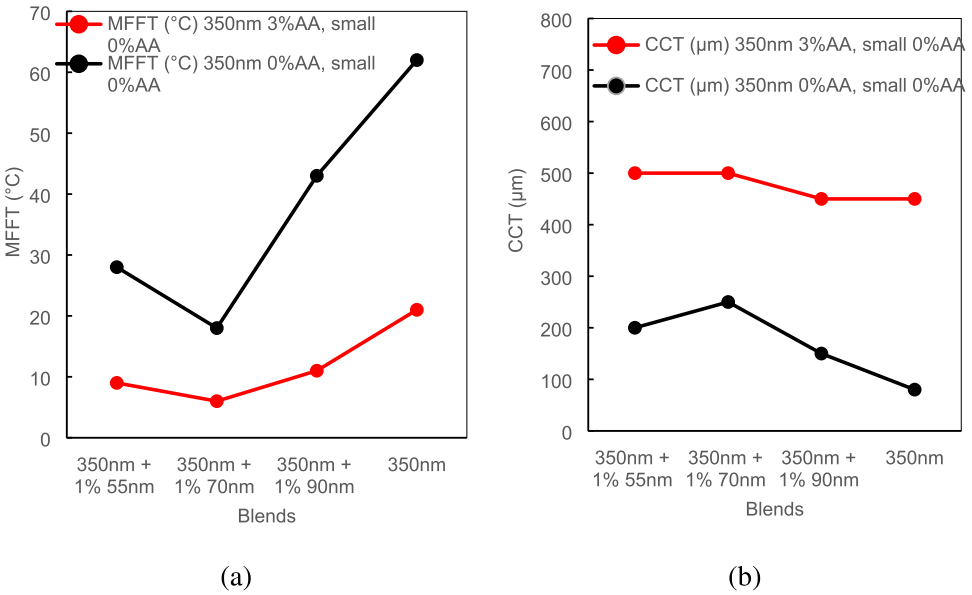

(a) (b)

Figure 1. Effect of adding 1 wt % of small particles with 55, 70, and 90 nm of diameter (latexes 1, 3, and 5) to a 350 nm latex with (latex 8) and without (latex 9) AA on (a) MFFT and (b) CCT.

between stress at break and elongation that results in tough films. However, MFFT increased and the CCT decreased with the particle size. On the other hand, higher contents of the hard phase led to stronger films, but they had high MFFT and low CCT. Although there is room for some improvement and these latexes can be further optimized by tuning the T_g and polymer architecture of the soft and hard polymers, these results show the limits of the technology.

This article is an attempt to go beyond these limits using blends of soft core–hard "shell" particles of different sizes. This strategy is somehow inspired by the work of Peters et al.,[20] who found that 75/25 (wt/wt %) blends of large and small homogeneous particles gave an MFFT that was significantly lower than those of the individual components of the blend. Similar results have been recently reported for blends of large and small hard core–soft shell particles.[21] Based on these results, we wondered if the MFFT could be reduced and CCT increased by adding low quantities of small particles to dispersions of large particles. The reason for limiting the amount of small particles is to reduce the total amount of surfactant and therefore the water sensitivity of the resulting films.

EXPERIMENTAL SECTION

Materials. Soft core–hard "shell" latexes of different particle size, acrylic acid (AA) content, and hard-phase content were synthesized by means of a two-stage semicontinuous seeded emulsion polymerization, following the procedure detailed in ref 17. Table 1 summarizes the soft core–hard "shell" latexes synthesized. In addition, pure poly(methyl methacrylate) and poly(butyl acrylate) latexes of 55 nm in diameter were prepared. The solid content of all latexes was 45 wt %.

Characterization. The average particle diameter (dp) was measured by dynamic light scattering (DLS) using a Zetasizer Nano Z (Malvern Instruments). The minimum film forming temperature (MFFT) was measured by casting the latexes on a temperature gradient bar (Rhopoint-Model 90) using a range of temperatures between 5 and 40 °C. The MFFT was observed visually as the point where the film became optically clear without visible cracks.

Critical cracking thickness (CCT) is the thickness at which the layer starts to crack. CCT was measured using a device made of anodized aluminum that has a thickness gradient between 0 and 2000 μm.[17] The device is filled with latex, and upon drying, the critical cracking thickness was determined visually at the point where the cracking started.

The stress evolution during film formation was examined via the beam bending technique.[17] Simultaneously, with the measurement of the stress, the rate of drying was determined gravimetrically using a Sartorius Entris 124-1S analytical balance (resolution 0.1 mg).

https://doi.org/10.1021/acs.macromol.3c01916
Macromolecules 2023, 56, 9054−9061

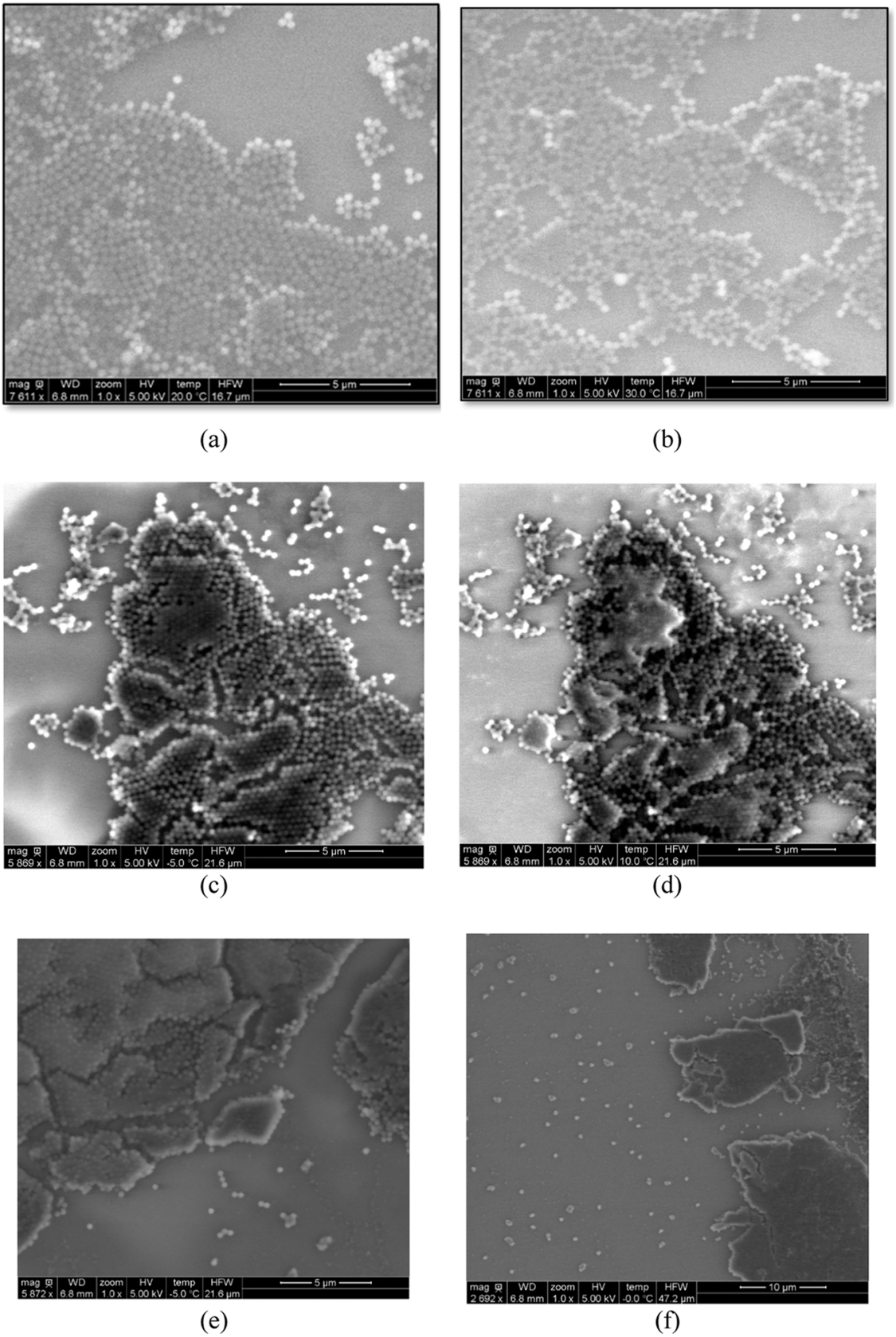

Figure 2. ESEM images of latex 9 (350 nm) and blends of latex 9 and latex 3 (70 nm), both of which are devoid of AA. (a) Latex 9 at 20 °C, (b) latex 9 at 30 °C, (c) latex 9 with 1 wt % of latex 3 at −5 °C, (d) latex 9 with 1 wt % of latex 3 at 10 °C, (e) latex 9 with 3 wt % of latex 3 at −5 °C, and (f) latex 9 with 3 wt % of latex 3 at 0 °C.

https://doi.org/10.1021/acs.macromol.3c01916
Macromolecules 2023, 56, 9054−9061

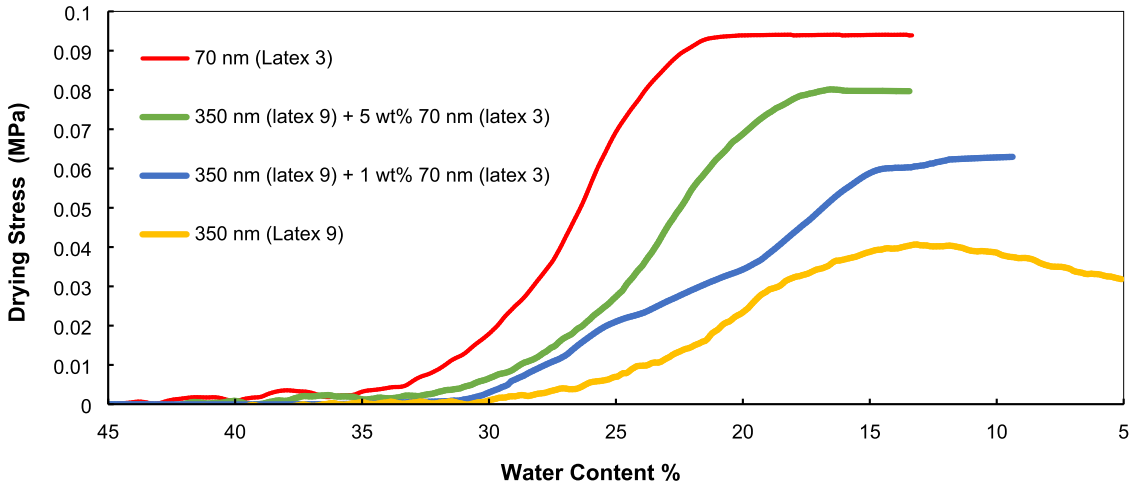

Figure 3. Evolution of the stress generated during film formation. One and 5 wt % of latex 3 (70 nm) was blended to latex 9 (350 nm).

Tensile tests were carried out as detailed in ref 17.

Environmental scanning electron microscopy (ESEM) images were acquired on a Quanta 250 FEG ESEM (FEI, Netherlands) equipped with a Peltier cooling stage and a GSE detector. Particle coalescence was studied following the procedure detailed in ref 22.

Water uptake of the films, dried from the latexes, was measured. The films were cast on silicone molds and had a dry thickness of 250 μm. After drying for 7 days at 23 °C/55% RH, the samples were weighed ($w1$) before immersing in water for 72 h. After that, the samples were dried with paper and then weighed again ($w2$). Water uptake % was calculated as follows

$$\text{Water Uptake \%} = \frac{w2 - w1}{w1} \times 100 \quad (1)$$

RESULTS AND DISCUSSION

As a benchmark for checking the effect of blending, the most demanding conditions were tested. The largest latex (350 nm, devoid of AA; latex 9), which gave the highest MMFT and the lowest CCT, was blended with only 1 wt % of smaller latexes (55, 70, and 90 nm also devoid of AA, latexes 1, 3, and 5). All of the blends were stable. It is worth pointing out that no stratification is expected for a 45 wt % solid content with size ratios (large/small) smaller than 7 and 1 wt % of small particles.[23] On the other hand, for 45 wt % of the solid latex, the average interparticle distance for 350 nm particles is given by

$$\text{IPD} = dp\left(\frac{0.64}{solids\ content}\right)^{1/3} = 43\ \text{nm} \quad (2)$$

This means that the 70 nm small particles should be accommodated in the interstitial sites between particles. Examples of this arrangement have been reported.[24,25]

Figure 1 presents the CCT and MFFT results of the blends. The values for the 350 nm latex (latex 9) are included for comparison. It can be seen that the MFFT is substantially reduced by adding only 1 wt % of the small latex. Thus, MFFT decreased from 62 °C (for the 350 nm latex) to 43 °C, adding only 1 wt % of the 90 nm latex, and down to 18 °C when 1 wt % of the 70 nm latex was added. In parallel, the CCT increased from 80 to 150 μm when 1 wt % of the 90 nm latex was added and to 250 μm for 1 wt % of the 70 nm latex. Figure 1 also shows that similar results were obtained for the 350 nm latex containing 3% of AA (latex 8), but due to the hydroplasticization effect,[17] the MFFTs were lower and the CCT was higher than those for the 350 nm latex devoid of AA. Higher concentrations of the small latexes led to further decrease of the MFFT and increase of the CCT (Table S1).

It is remarkable that the MFFT increased, and the CCT decreased when the size of the small particles was further decreased to 55 nm. In this regard, it is worth pointing out that for blends of the 250 nm latexes with 1 wt % of smaller latexes (55 and 70 nm), the best results were obtained in blends with the 55 nm latex (Table S2). This suggests that there may be an optimal ratio between the sizes of the large and small particles, which is close to five. For 1 wt % of small particles, this ratio results in a similar number of small and large particles (particles/interstitial gaps = 1.2). It is worth pointing out that while the AA content of the large particles strongly affected the results, the AA content of the small particles had only a small effect (Figure S1).

It is surprising that only 1 wt % of the small latex could produce such a significant effect. In order to investigate this phenomenon, the effect of the presence of small particles on film formation was investigated by environmental scanning electron microscopy (ESEM). Figure 2 shows that the 350 nm particles (latex 9) maintained their identity at 30 °C (Figure 2a,b), adding only 1 wt % of 70 nm particles (latex 3) was enough to force sintering of particles at 10 °C (Figure 2c,d), and this temperature was further reduced to 0 °C when 3 wt % of the 70 nm latex was used (Figure 2e,f). This demonstrated that the presence of a tiny fraction of small particles facilitates the deformation of the large particles, which likely reduces the generation of stress during film formation.

In order to check this point, the stress generated during film formation was determined via the beam bending technique. Figure 3 shows the evolution of the stress for films cast from blends of 350 (latex 9) and 70 nm latexes (latex 3), both devoid of AA. The stresses for the individual latexes are included for comparison. It can be seen that contrary to the expectations, the presence of small particles resulted in an increase in the stress generated during film formation, but no cracks were formed, whereas cracking was observed for the 350 nm latex, as evidenced by the decrease of the stress that is a fingerprint of cracking. These results suggest that the reason for the higher resistance of the films cast from the blends was an increase in their cohesion. One may speculate that this is the result of an increase in the number of contact points due to the presence of small particles. Another possibility, suggested by the ESEM

https://doi.org/10.1021/acs.macromol.3c01916
Macromolecules 2023, 56, 9054−9061

Time	(a) Large particles only (350 nm)		(b) Large articles (350 nm) with an interstitial small particle (70 nm)	
	illustration	Max. deforming stress (Pa)	illustration	Maximum deforming stress (Pa)
≅ Zero Sec	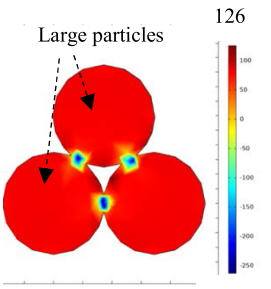	263	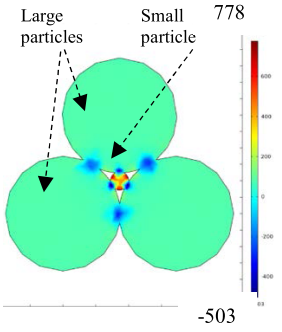	503
≅ 20 Sec	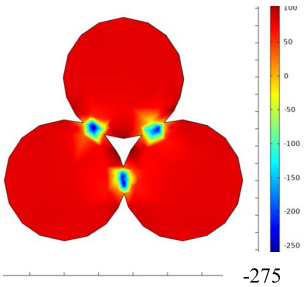	275	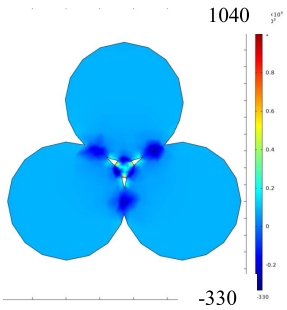	330
≅ 40 Sec	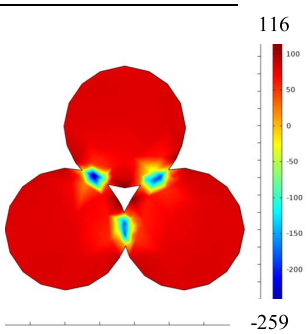	259	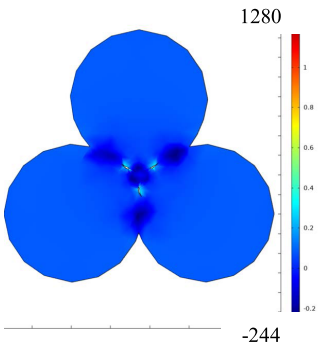	244
≅ 150 Sec	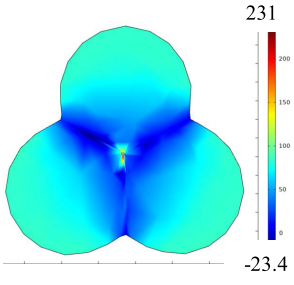	23.4		

Figure 4. Effect of the presence of 70 nm soft core−hard "shell" particles on the deformation of 350 nm soft core−hard "shell" particles immersed in water.

results, is that the higher deformation led to an increase in the overall contact area between particles.

It can be speculated that the reasons for the increase in stress are linked to the decrease in the radius of curvature of the

https://doi.org/10.1021/acs.macromol.3c01916
Macromolecules 2023, 56, 9054−9061

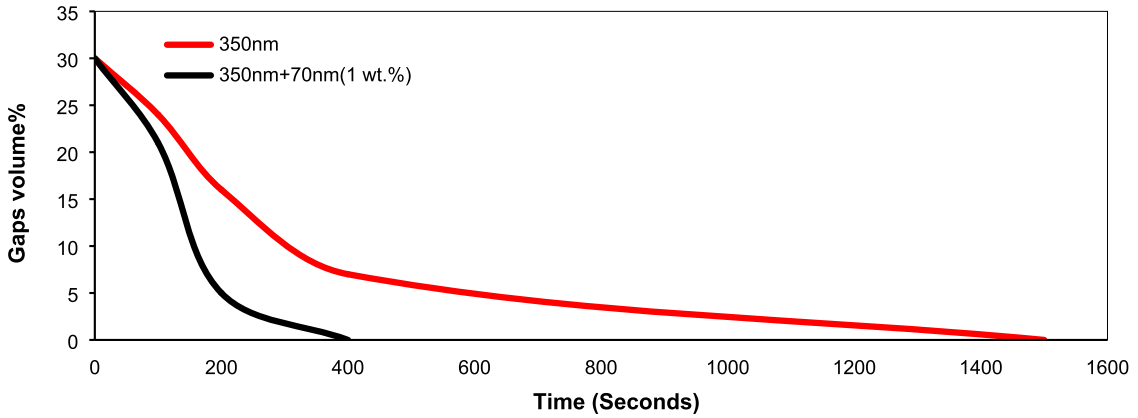

Figure 5. Effect of the presence of 1 wt % of 70 nm soft core−hard "shell" particles (latex 3) on the reduction of the volume of the gaps between 350 nm soft core−hard "shell" particles (latex 9).

Table 2. Effect of the Viscoelastic Properties of the Small Particles[a]

fraction of small particles	PMMA MFFT (°C)	PMMA CCT (μm)	PBA MFFT (°C)	PBA CCT (μm)
0.5 wt %	62	70	62	80
1 wt %	58	85	62	80
2 wt %	63	50	60	80
4 wt %	68	50	55	120
10 wt %	>70	≅0	21	200

[a]Blends of latex 9 (350 nm) with 55 nm particles of PMMA and PBA.

Table 3. Effect of the Addition of 1 wt % of 70 nm Particles on the Tensile Strain Curve of Films Formed with 350 nm Particles (with and without AA)

latex	Young's modulus (MPa)	stress at Break (MPa)	elongation at break (%)	toughness (MPa)
latex 9 (350 nm, no AA)	3.0	10.3	130	9.2
latex 9 + 1 wt % of latex 3 (70 nm, no AA)	2.7	8.9	257	16.1
latex 8 (350 nm, AA 3%)	2.7	7.1	160	8.6
latex 8 + 1 wt % of latex 3 (70 nm, no AA)	1.9	7.4	280	14.5

menisci, resulting in an increase in Laplace pressure, which accelerated the deformation of the viscoelastic particles. In order to check this hypothesis, the sintering of 350 nm particles with and without one interstitial 70 nm particle was simulated. The Navier−Stokes equations were modified to account for the viscoelasticity of the particles and solved using COMSOL Multiphysics version 5.6 (information given in the Supporting Information). Homogeneous particles were used for simplification. Figure 4 presents the evolution of the sintering and the values of the deforming stresses. It can be seen that the presence of the small particle almost doubled the value of the particle deforming stress. This phenomenon is linked to the decrease of the contact angle between particles that increased the Laplace pressure. This accelerated and facilitated the deformation of the viscoelastic particles. As a result of the higher deformation stress, the 350 nm particles deformed faster in the presence of the 70 nm particles (Figure 5).

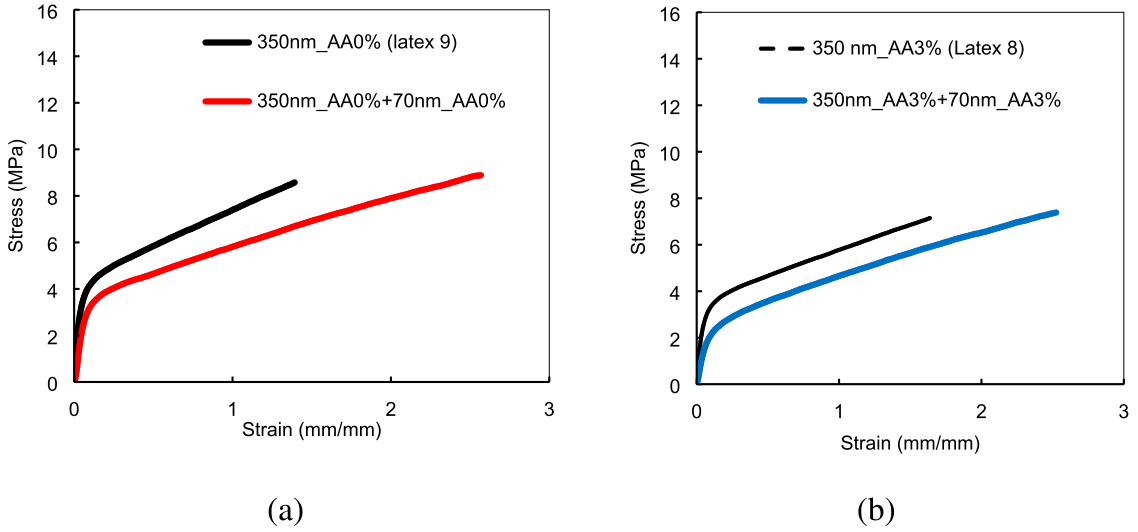

Figure 6. Effect of the addition of 1 wt % of 70 nm particles on the tensile strain curve of films formed with 350 nm particles. (a) Latex 9 (350 nm, without AA) with 1 wt % of latex 3 (70 nm, without AA) and (b) latex 8 (350 nm, 3% AA) with 1 wt % of latex 2 (70 nm, 3% AA).

https://doi.org/10.1021/acs.macromol.3c01916
Macromolecules 2023, 56, 9054−9061

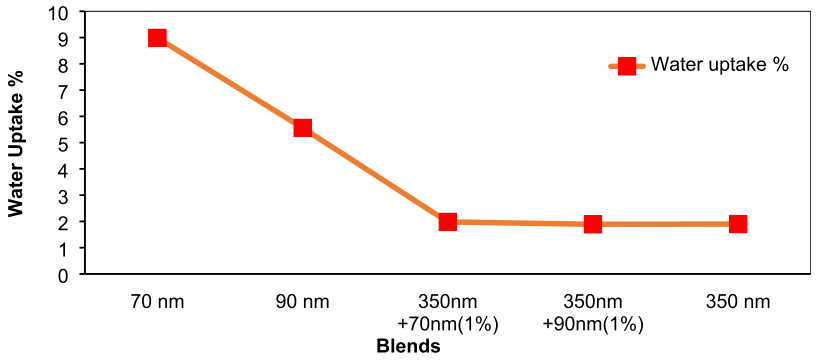

Figure 7. Water uptake of films prepared from monomodal latexes and blends devoid of AA after immersion in water for 3 days of immersion in water.

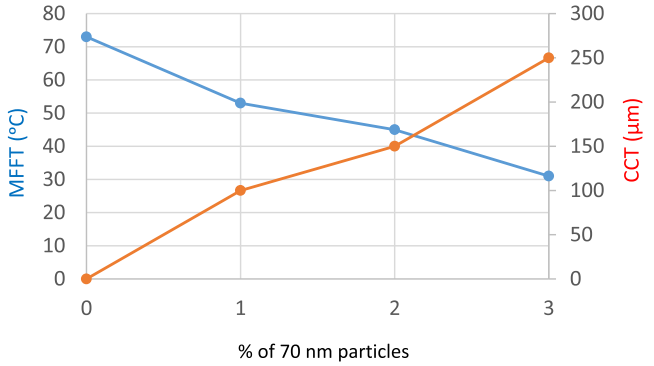

Figure 8. Effect of adding 70 nm particles (latex 3) to a hard large latex (latex 10, 30 wt % of hard phase, diameter: 359 nm) on MFFT and CCT.

Experimental results and model predictions support the hypothesis that the presence of small particles facilitates the deformation of particles. In this context, the viscoelastic properties of the small particles might have an effect. To investigate this point, latex 9 (350 nm, devoid of AA) was blended with different fractions of 55 nm latexes of different glass transition temperatures (poly(butyl acrylate) (PBA, T_g = −54 °C) and poly(methyl methacrylate) (PMMA), T_g = 110 °C). The results are presented in Table 2, where it can be seen that the small PMMA and PBA latexes behaved as hard and soft fillers, respectively, without any significant effect for small fractions of the small particles. The volume fraction of the small particles was lower than that required to form a continuous phase in the film.[24] The results in Table 2 indicate that in order to have a significant effect, the small latex should have viscoelastic properties similar to the large one.

The results presented above suggest that the film formation behavior of a large particle latex can be substantially improved by adding only 1 wt % of small particles of similar viscoelastic properties. However, this would not be useful if it were accompanied by a detriment in the mechanical properties. Figure 6 and Table 3 present the effect of blending on the tensile tests. It can be seen that both in the presence and in the absence of AA, blending has a positive effect on the mechanical properties of the films. Blending slightly reduced the Young's modulus and had almost no effect on the maximum strength, while it increased the maximum strain and the film toughness. Therefore, blending with 1 wt % of small particles improved both film formation and mechanical properties.

One of the limitations of using small particles is that they contain higher surfactant contents, which leads to a higher water sensitivity. Therefore, it is important to check the effect of blending on water uptake. Figure 7 shows that the addition of 1 wt % of 70 nm particles with 0 wt % AA had nearly no effect on the water sensitivity of the film after 3 days of immersion in water.

In ref 17, it was shown that the increase of the hard phase content from 25 to 30 wt % led to a severe increase of the MFFT and to a strong decrease of the CCT, limiting the usefulness of this latex. Table 4 and Figure 8 shows that the addition of low amounts of small particles to a larger latex having a high amount of hard phase (latex 10, 30 wt % of hard phase, diameter: 359 nm) resulted in a substantial reduction of the MFFT and an important increase in CCT. This broadens the range of hard phase/soft phase ratios that can be used.

CONCLUSIONS

This article shows that the addition of tiny amounts of small particles (e.g., 1 wt %) leads to a substantial improvement of both film formation (strong decrease of MFFT and increase of CCT) and mechanical properties (higher elongation at break and toughness, slightly reducing the Young's modulus and maintaining the stress at break), without any effect on the water sensitivity of the film. It was found that there is an optimal ratio between the sizes of the large and small particles, which is close to five. An important finding is that in order to have a significant effect, the small particles should have similar viscoelastic properties as the large ones. Furthermore, the addition of small particles allows one to use high contents of the hard phase, broadening the range of hard phase/soft phase ratios that can be used.

ASSOCIATED CONTENT

Supporting Information

The Supporting Information is available free of charge at https://pubs.acs.org/doi/10.1021/acs.macromol.3c01916.

Effect of the amount of 55 nm particles (latex 1) added to 350 nm particles (latex 9) on MFFT and CCT. Effect of the addition of 1 wt % of small particles of 55 and 70 nm to big particles of 250 nm (latex 7). Effect of the AA content of the small particles on the MFFT and CCT. Model for particle deformation (PDF)

AUTHOR INFORMATION

Corresponding Author

José M. Asua − *POLYMAT and Departamento de Química Aplicada, Facultad de Ciencias Químicas, University of the Basque Country UPV/EHU, Donostia-San Sebastian 20018,*

https://doi.org/10.1021/acs.macromol.3c01916
Macromolecules 2023, 56, 9054−9061

Spain; orcid.org/0000-0002-7771-1543;
Email: jm.asua@ehu.eus

Authors

Hesham Abdeldaim − *POLYMAT and Departamento de Química Aplicada, Facultad de Ciencias Químicas, University of the Basque Country UPV/EHU, Donostia-San Sebastian 20018, Spain*

Edurne González − *POLYMAT and Departamento de Química Aplicada, Facultad de Ciencias Químicas, University of the Basque Country UPV/EHU, Donostia-San Sebastian 20018, Spain*

Noé Duarte − *Nanoscience research center CIC nanoGUNE, San Sebastian 20012 Basque Country, Spain*

Complete contact information is available at:
https://pubs.acs.org/10.1021/acs.macromol.3c01916

Notes

The authors declare no competing financial interest.

■ ACKNOWLEDGMENTS

The authors would like to acknowledge the financial support provided by the Industrial Liaison Program in Polymerization in Dispersed Media (Akzo Nobel, Allnex, Arkema, Asian Paints, BASF, Covestro, Elix Polymers, Inovyn, Organik Kimya, Sherwin Williams, Stahl, Synthomer, Tesa, Vinavil and Wacker). In addition, the authors would also like to acknowledge Dr. Andrey Chuvilin and Dr. Christopher Tollan for their help and support with the ESEM measurements.

■ REFERENCES

(1) Bender, R.; Féron, R.; Mills, D.; Ritter, S.; Bäßler, R.; Bettge, D.; De Graeve, I.; Dugstad, A.; Grassini, S.; Hack, T.; Halama, M.; Han, E.; Harder, T.; Hinds, G.; Kittel, J.; Krieg, R.; Leygraf, C.; Martinelli, L.; Mol, A.; Neff, D.; Nilsson, J.; Odnevall, I.; Paterson, S.; Paul, S.; Prošek, T.; Raupach, M.; Revilla, R. I.; Ropital, F.; Schweigart, H.; Szala, E.; Terryn, H.; Tidblad, J.; Virtanen, S.; Volovitch, P.; Watkinson, D.; Wilms, M.; Winning, G.; Zheludkevich, M. Corrosion challenges towards a sustainable society. *Mater. Corros.* **2022**, *73*, 1730−1751.

(2) Halleux, V. Revision of the industrial emissions directive. *Eur. Ind. Emiss. Directive* **2022**, 733−570.

(3) Winnik, M. A.; Pinenq, P.; Krüger, C.; Zhang, J.; Yaneff, P. V. Crosslinking vs. interdiffusion rates in melamine-formaldehyde cured latex coatings: a model for waterborne automotive basecoat. *J. Coat. Technol.* **1999**, *71*, 47−60.

(4) González, I.; Asua, J. M.; Leiza, J. R. Crosslinking in acetoacetoxy functional waterborne crosslinkable latexes. *Macromol. Symp.* **2006**, *243*, 53−62.

(5) Kessel, N.; Illsley, D. R.; Keddie, J. L. The diacetone acrylamide crosslinking reaction and its influence on the film formation of an acrylic latex. *J. Coat. Technol. Res.* **2008**, *5*, 285−297.

(6) Chen, Y.; Jones, S. T.; Hancox, I.; Beanland, R.; Tunnah, E. J.; Bon, S. A. F. Multiple hydrogen-bond array reinforced cellular polymer films from colloidal crystalline assemblies of soft latex particles. *ACS Macro Lett.* **2012**, *1*, 603−608.

(7) González, E.; Paulis, M.; Barandiaran, M. J. Effect of controlled length acrylic acid-based electrosteric stabilizers on latex film properties. *Eur. Polym. J.* **2014**, *59*, 122−128.

(8) Musa, M. S.; Milani, A. H.; Shaw, P.; Simpson, G.; Lovell, P. A.; Eaves, E.; Hodson, N.; Saunders, B. R. Tuning the modulus of nanostructured ionomer films of core−shell nanoparticles based on poly(n-butyl acrylate). *Soft Matter* **2016**, *12*, 8112−8123.

(9) Jiménez, N.; Ballard, N.; Asua, J. M. Hydrogen bond-directed formation of stiff polymer films using naturally occurring polyphenols. *Macromolecules* **2019**, *52*, 9724−9734.

(10) Ballard, N. Supramolecularly reinforced films from polyuethane-urea dispersions containing the tris-urea motif. *ACS Appl. Polym. Mater.* **2020**, *2*, 4045−4053.

(11) Argaiz, M.; Ruipérez, F.; Aguirre, M.; Tomovska, R. Ionic interparticle complexation effect on the performance of waterborne coatings. *Polymers* **2021**, *13*, 3098.

(12) Dos Santos, F. D.; Fabre, P.; Drujon, X.; Meunier, G.; Leibler, L. Films from soft-core/hard-shell hydrophobic latexes: structure and thermomechanical properties. *J. Polym. Sci., Part B: Polym. Phys.* **2000**, *38*, 2989−3000.

(13) Dos Santos, F. D.; Leibler, L. J. Large deformation of films from soft-core/hard-shell hydrophobic lattices. *Polym. Sci., Part B: Polym. Phys.* **2003**, *41*, 224−233.

(14) Price, K.; Wu, W.; Wood, K.; Kong, S.; McCormick, A.; Francis, L. Stress development and film formation in multiphase composite latexes. *J. Coat. Technol. Res.* **2014**, *11*, 827−839.

(15) Schuler, B.; Baumstark, R.; Kirsch, S.; Pfau, A.; Sandor, M.; Zosel, A. Structure and properties of multiphase particles and their impact on the performance of architectural coatings. *Prog. Org. Coat.* **2000**, *40*, 139−150.

(16) Limousin, E.; Ballard, N.; Asua, J. M. Soft core−hard shell latex particles for mechanically strong VOC-free polymer films. *J. Appl. Polym. Sci.* **2019**, *136*, 47608.

(17) Abdeldaim, H.; Reck, B.; Roschmann, K. J.; Asua, J. M. Cracking in films cast from soft core/hard shell waterborne dispersions. *Macromolecules* **2023**, *56*, 3304−3315.

(18) Abdeldaim, H.; Asua, J. M. Modelling cracking during film formation of soft core/hard shell latexes. *Chem. Eng. J.* **2023**, *473*, No. 145270.

(19) Yow, H. N.; Goikoetxea, M.; Goehring, L.; Routh, A. F. Effect of film thickness and particle size on cracking stresses in drying latex films. *J. Colloid Interface Sci.* **2010**, *352*, 542−548.

(20) Peters, A. C. I. A.; Overbeek, G. C.; Buckmann, A. J. P.; Padget, J. C.; Annable, T. Bimodal dispersions in coating applications. *Prog. Org. Coat.* **1996**, *29*, 183−194.

(21) Brito, E. L.; Ballard, N. Film formation of hard-core/soft-shell latex particles. *J. Polym. Sci.* **2023**, 410−421.

(22) Gonzalez, E.; Tollan, C.; Chuvilin, A.; Barandiaran, M. J.; Paulis, M. Determination of the coalescence temperature of latexes by environmental scanning electron microscopy. *ACS Appl. Mater. Interfaces* **2012**, *4*, 4276−4282.

(23) Makepeace, D. K.; Fortini, A.; Markov, A.; Locatelli, P.; Lindsay, C.; Moorhouse, S.; Lind, R.; Sear, R. P.; Keddie, J. L. Stratification in binary colloidal polymer films: experiment and simulations. *Soft Matter* **2017**, *13*, 6969−6980.

(24) Tzitzinou, A.; Keddie, J. L.; Geurts, J. M.; Peters, A. C. I. A.; Satguru, R. Film formation of latex blends with bimodal particle size distributions. Consideration of particles deformability and continuity of the dispersed phase. *Macromolecules* **2000**, *33*, 2695−2708.

(25) Ballard, N.; Urrutia, J.; Eizaguirre, S.; Schäfer, T.; Diaconu, G.; de la Cal, J. C.; Asua, J. M. Surfactant kinetics and their importance in nucleation events in (mini)emulsion polymerization revealed by quartz crystal microbalance with dissipation monitoring. *Langmuir* **2014**, *30*, 9053−9062.